Salinity Management in the World's Most Saline Dam Reservoir: The Gotvand Reservoir, Iran

Siamak Amiri[1], Mehdi Mazaheri[1,*], Vahid Naderkhanloo[1], Jamal Mohammad Vali Samani[1], Sahand Ghadimi[2], Ali Torabi Haghighi[2], Roohollah Noori[3,4,*]

[1]Department of Water Engineering and Management, Tarbiat Modares University, P.O. Box 14115-336, Tehran, Iran.

[2]Water, Energy, and Environmental Engineering Research Unit, University of Oulu, P.O. Box 4300, FIN-90014 Oulu, Finland.

[3]Graduate Faculty of Environment, University of Tehran, Tehran, 1417853111, Iran.

[4]Faculty of Governance, University of Tehran, Tehran, 1439814151, Iran.

***Corresponding authors:** Mehdi Mazaheri (m.mazaheri@modares.ac.ir), ORCID: https://orcid.org/0000-0001-8670-1710 and Roohollah Noori (noor@ut.ac.ir), ORCID: http://orcid.org/0000-0002-7463-8563

Key Points:

- A modeling approach was used to manage salinity in the world's most saline dam reservoir, i.e., the Gotvand reservoir, Iran.
- Pycnocline established in the early impoundment stage lasted during the study period, leading to a crenogenic meromixis in the reservoir.
- Findings show that reservoir salinity management could mitigate outlet salinity and preserve downstream environment from salinity hazards.

Abstract

The Gotvand dam was built on the most important Iranian river to support a number of populated cities with freshwater, provide irrigation water for million hectares of fertile farmlands, and meet water demand for the country's hub industrial zones. This dam is known as one of the worst engineering failures in Iran's history because its impoundment submerged the enormous salty unit of Gachsaran evaporite formation (GEF) outcropped in the reservoir, leading to reservoir water salinization in deep layers up to several times greater than that of in the high-seas. Given the failed practical application of direct intervention strategies to control the salinity crisis, we suggested a low-cost salinity management strategy based on the reservoir operation to mitigate the dam outlet salinity and preserve the downstream environment from the salinity hazards. The three-dimensional MIKE3 model, was run to calculate the GEF dissolution rate, accumulated salt in the reservoir, and the dam outlet salinity. Then, we ran the model considering different outlet salinity levels to explore the best reservoir operation strategy to prohibit the accumulated salt in the reservoir and keep the safe salinity for downstream irrigation-use. Simulation results suggested that the GEF dissolution rate varied from 0.5 to 7 cm/hr, mainly due to incremental submergence of the GEF during multi-stage impoundment of the reservoir. Considering the final dissolution rate of 0.5 cm/hr and inlet salinity from the upstreams, salt accumulation inside the reservoir can be gradually prevented by setting the outlet salinity to its maximum historical downstream level, i.e., 1400 µmhos/cm.

1 Introduction

Dam construction has always been a major engineering solution in both industrialized and developing countries to mitigate hydrologic hazards, supply anthropogenic water demands, and promote human welfare and development (Simonovic and Arunkumar, 2016; Best, 2019; Winton et al., 2019; Mulligan, 2020). However, many of these hydro systems have encountered environmental and economic failure due to, among other things, eutrophication (Zaragüeta and Acebes, 2017; Noori et al., 2021), sedimentation (Wang and Kondolf, 2014), and reservoir water salinization (Kerachian and Karamouz, 2007; Tavoosi et al., 2022). Reservoir water salinization is mainly associated with the submerged salty unit of evaporite formations and saline tributaries (Jalali et al., 2019). Outcropped saline geological formations in reservoir areas have critical implications for reservoir water quality, dam structures, and the downstream ecosystems, which may prohibit the dams from (in some cases) no longer being able to fulfill their purposes (Poff et al., 2016; Winton et al., 2019). Therefore, reservoir salinity management is required to mitigate the negative impacts of water quality and potential downstream environmental consequences.

The Gotvand dam, the greatest mistake in the history of Iranian engineering, was built on the country's most important river, i.e., Karun River, in a region with an outcropped salty unit of geological formations (mainly, Gachsaran evaporite formation – GEF) in 2011. Due to the Gotvand reservoir impoundment, vast GEF within the reservoir area was submerged, making the reservoir water increasingly saline. The salinity of the reservoir water in the bottom layers has reached up to several times higher than the salinity of the high-seas (Aghasian et al., 2019), establishing the Gotvand as the world's most saline drinking water reservoir (based on our knowledge). Therefore, if adequate and necessary measures are not considered to control the reservoir water outlet immediately, salinization would threaten the dam reservoir and the downstream environment that consists of million hectares of fertile agricultural lands, Iran's hub industrial zones, populated cities and unique protected areas (Naderkhanloo, 2013; Fakouri et al., 2019; Malek Mohammadi et al., 2022). In the face of the present problem, different managerial strategies were outlined, as summarized in Table S1. These strategies can be divided into (i) direct intervention strategies that rely on fundamental physio-environmental changes (e.g., carrying salt masses out of the reservoir, disconnecting the reservoir water from salt masses by coating such as geo-membrane, building a clay blanket to decelerate the dissolution rate, and laying transmission pipelines in the reservoir bottom to convey salinity to the Persian Gulf), and (ii) practices of crisis management including reservoir water salinity management without performing any remedial operations (IPRC, 2011; MGCEC, 2012). Given the direct intervention strategies proving ineffective or having adverse effects, the low-cost management and operation of the dam reservoir is a viable alternative to reduce reservoir outlet salinity without further interventions in the downstream environment. These management-based practices aim to resolve the existing problem with maximum final performance and minimum execution and operational interference (IPRC, 2011; MGCEC, 2012; Aghasian et al., 2019). They typically have fewer consequences and costs, both economically and operationally (Naderkhanloo, 2013; Aghasian et al., 2019).

This study developed a useful management-based strategy using the MIKE3 model to control and resolve the salinity crisis at the Gotvand dam reservoir under current deteriorating conditions. From the viewpoint of geometry, topography, and the presence of GEF, the Gotvand reservoir is a complex water body with the outcropped GEF in different parts of the reservoir area in triple directions of *x*, *y*, and *z*. Therefore, we modelled the GEF as the salinity source that affects both the plan (*x* and *y* directions) and the reservoir's depth (*z* direction). Given that the MIKE3 model is not simply sophisticated to deal with nonpoint sources of pollution, such as the outcropped evaporite formations, we introduced the GEF to the model as a collection of point sources. Another challenge in introducing the GEF into the mathematical model is our poor understanding of the GEF dissolution rate (Aghasian et al., 2019) – this important parameter varies in both space and time. In general, it is not recommended to use the suggested dissolution rates for different evaporite formations due to the high range of uncertainty reported in the related studies conducted globally (Raines and Dewers, 1997; Klimchouk and Aksem, 2002; Baghdardokht and Heidari, 2005; Aljubouri and Al-Kawaz, 2007; Mbogoro et al., 2011; Valor et al., 2011; Lebedev, 2015; Domínguez-Villar et al., 2017; Feng et al., 2017; Hong et al., 2018; Tang et al., 2018; Tavoosi et al., 2022). The exact solution to understand the GEF dissolution rate in lakes/reservoirs is through laboratory tests or field measurements. In the case of the Gotvand reservoir, it was difficult to determine the exact dissolution rate due to the impossibility of physical models that incorporate natural conditions in the process. Here, we estimated the GEF dissolution rate using salinity calibration of the mathematical model in the Gotvand reservoir. Contrary to similar studies (e.g., Aghasian et al., 2019; Tavoosi et al., 2022), we considered the GEF dissolution rate as a space-time dependent variable in the model to appropriately highlight the impact of different impoundment stages on the GEF dissolution in the reservoir.

Everything considered, we examined how water extraction conditions from different levels of the Gotvand hypersaline dam reservoir simultaneously affect reservoir water salinity and downstream of the dam. Our findings revealed that the undesirable impact of the GEF on the reservoir will persist for a period in the future. However, salt mass volume will decrease due to its continuous dissolution over time.

2 Study area

2.1. General description

Gotvand, with a height of 182 m, is the tallest Iranian embankment dam. It is located at 32° 15' 59" N and 48° 55' 51" E, northeast of Gotvand city, Khuzestan province, in southwest Iran. This dam, with a storage capacity of around 4.7 km^3 at the normal operating level, was built about 380 km away from the Karun's river mouth at the Persian Gulf in 2011 (Fig. 1a) (IPRC, 2011; IWPRDC, 2011; MGCEC, 2012; Jalali et al., 2019). Karun is the largest and most important river in Iran, with a crucial role in hydropower generation and water supply for irrigation, industry, and sanitary uses. Five dams are constructed along this river, with a total storage capacity of around 13.1 km^3, making it the most regulated river in Iran. The Gotvand is the last (location-wise) constructed dam on this river (IWPRDC, 2011; Aghasian et al., 2019; Fakouri et al., 2019). It was constructed to increase the country's energy production capacity and promote its international position in terms of energy security, indigenization of related technologies, flood control, water supply for different uses (especially drinking water for urban residents), and social welfare of the surrounding region (IWPRDC, 2011). The highest rate of hydroelectric power generation in Iran belongs to this dam (4250 GWh per year). Compared to the other related industries involved in the Gotvand project, farmers' position seems far more sensitive since a million hectares of farmlands and thousands of farming operators exist downstream.

Detailed information about the course of development and social, political, and environmental effects connected to the Gotvand dam project is given in Text S1.

2.2. The reservoir salinization

During the impoundment phase of the Gotvand dam, the vast and large GEF within the reservoir (Fig. 1) began to dissolve, making it increasingly saline. The GEF extends 4.5 km upstream from the dam axis (Figs. 1b to 1d) (MGCEC, 2012). Measurements demonstrate that the degree of water salinity, in terms of electrical conductivity (EC), at 11 km from the Gotvand downstream is nearly 1200 μmhos/cm. However, the salinity of dam outlet water is still at an optimum level compared to the desired maximum level (1650 μmhos/cm), allowing a maximum concentration for irrigation use (2500 μmhos/cm) (Naderkhanloo, 2013).

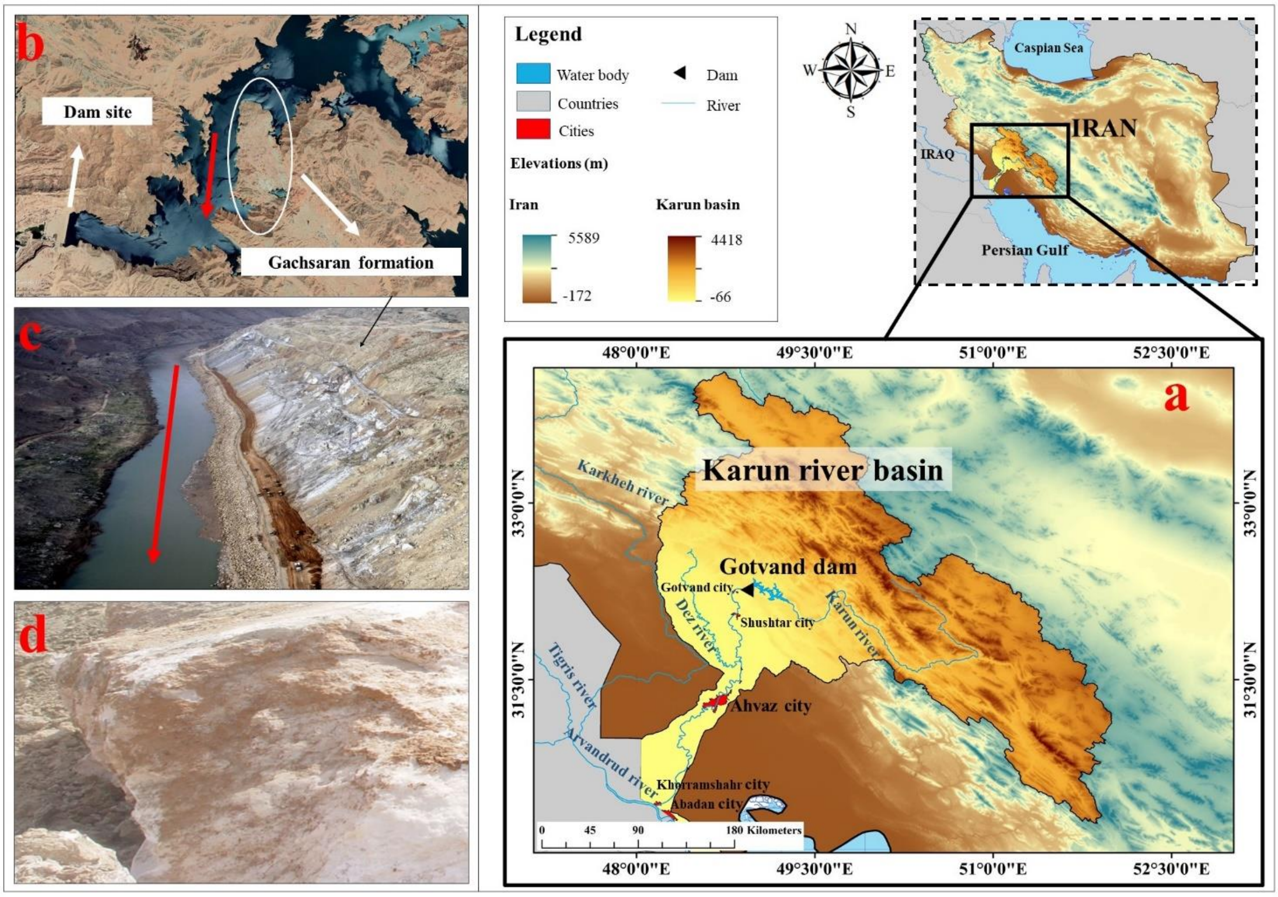

Figure 1. (a) The location of the Gotvand dam in the Karun river basin, Khuzestan province, Iran; and (b, c, and d) the location of the Gachsaran evaporite formation (GEF) on the left bank of the Gotvand dam reservoir.

To properly mitigate the negative impacts of the Gotvand reservoir impoundment, two salient points should be addressed: (i) the degree of water salinity downstream should be considered, and (ii) there is no guarantee that the outlet water maintains its optimum quality. Upon reservoir impoundment, the water level at the dam's location increased from 80-90 m (river water level) to 230 m above sea level (a.s.l) at the normal operating level. During this phase, the GEF, which mainly consists of gypsum, marl, and salt masses, at the left abutment of the dam (Fig. 1b) was partially submerged, and the dissolution process of salt was started. The GEF dissolution will proceed through four subsequent main mechanisms (IPRC, 2011):

- Dissolution of the outcropped GEF (scattered throughout the lateral surface of the reservoir) by its direct contact with reservoir water and causing free saline flow conveyance on this surface (simultaneously from the outset of impoundment),
- Dissolution of the GEF existing in the walls of karst cavities and its entry into the reservoir owing to concentration gradient (after the start of impoundment),
- Dissolution of the GEF and their entry into the reservoir simultaneously with a decline in water surface elevation arising from hydraulic gradient (peculiar to operation period),
- Dissolution of the GEF because of instability, fall, and partial slippage of masses into the reservoir (during operation and over the impoundment period, depending on the degree of salt dissolution).

In addition to the GEF, three small saline tributaries that join the Karun River at the Gotvand dam upstream (i.e., Murghab, Andika, and Lali tributaries) further contribute to reservoir salinization (Fig. S1 and Table S2). These tributaries are around 3 to 17 times more saline than the Karun river.

3 Numerical simulation

Thorough knowledge of flow hydrodynamics, salinity layering, and salt accumulation is needed to exert salinity management of reservoir water and explore its feasibility. Here, we outline the mathematical modelling stages and required data/parameters for the Gotvand reservoir salinity simulation. The mathematical model was set up for the Gotvand dam reservoir to call the primary data (hydrological, climatological, topographical, and water salinity data) and the constructed meshes. After that, the model was calibrated and verified based on water surface elevation and in-situ measured depth profiles of water temperature and salinity to ensure the model's performance. Finally, the tuned mathematical model was run for reservoir salinity stratification and accumulation and evaluating different salinity management scenarios in the dam downstream.

3.1. Salinity transport model and governing equations

In light of their dimensions, dam reservoir hydrodynamics and salinity distribution vary in lateral, vertical, and longitudinal directions. Given the complex geometry and topography of the Gotvand dam reservoir and the 3D distribution of the GEF in the reservoir area (see Figs. S2 and S3), we employed the mathematical model of MIKE3 to further investigate the salinity crisis in this reservoir. This model has been successfully applied for 3D simulation of hydrodynamics and water quality around the world (Bedri et al., 2014; Kheirabadi et al., 2018; Ranjbar et al., 2020 and 2022). MIKE 3 model can consider the entire evaporite formation face, which extends at the reservoir's depth as the salinity source. Additionally, the model determines the salinity concentration at different widths and depths of the reservoir and its outlets, leading to reliable outputs for the salinity management in Gotvand hypersaline reservoir.

In this study, only hydrostatic pressure was assumed, and the calculation of rotational currents in plan and depth and velocity changes were performed in three dimensions. The equations discussed above, thus, are presented as follows (DHI, 2017):

- Continuity equation

$$\frac{\partial u}{\partial x} + \frac{\partial v}{\partial y} + \frac{\partial w}{\partial z} = S \tag{1}$$

where, *x*, *y*, and *z* are the Cartesian coordinates in lateral, longitudinal, and vertical directions, respectively; *u*, *v*, and *w* represent the flow velocity components in the directions of *x*, *y*, and *z*, respectively; and *S* is the value of point source discharges.

- Momentum equations

Momentum equations along *x* and *y* axes are described as follows:

$$\frac{\partial u}{\partial t} + \frac{\partial u^2}{\partial x} + \frac{\partial vu}{\partial y} + \frac{\partial wu}{\partial z} = fv - g\frac{\partial \eta}{\partial x} - \frac{1}{\rho_0}\frac{\partial P_a}{\partial x} - \frac{g}{\rho_0}\int_z^\eta \frac{\partial \rho}{\partial x}dz - \frac{1}{\rho_0 h}\left(\frac{\partial s_{xx}}{\partial x} + \frac{\partial s_{xy}}{\partial y}\right) + F_u + \frac{\partial}{\partial z}\left(v_t\frac{\partial u}{\partial z}\right) + u_s S \tag{2}$$

$$\frac{\partial v}{\partial t} + \frac{\partial v^2}{\partial y} + \frac{\partial uv}{\partial x} + \frac{\partial wv}{\partial z} = -fu - g\frac{\partial \eta}{\partial y} - \frac{1}{\rho_0}\frac{\partial P_a}{\partial y} - \frac{g}{\rho_0}\int_z^\eta \frac{\partial \rho}{\partial y}dz - \frac{1}{\rho_0 h}\left(\frac{\partial s_{yx}}{\partial x} + \frac{\partial s_{yy}}{\partial y}\right) + F_v + \frac{\partial}{\partial z}\left(v_t\frac{\partial v}{\partial z}\right) + v_s S \tag{3}$$

where, *t* is the time. $h = \eta$+d, where η is the surface elevation, and *d* stands for the still water depth. $f = 2\Omega \sin \emptyset$ reflects the Coriolis force, where Ω is the angular revolution rate, and ϕ denotes the geographical latitude. Gravitational acceleration and water density are shown by g and ρ, respectively. s_{yy}, s_{yx}, s_{xy}, and s_{xx} are components of the radiation stress tensor. The vertical eddy (turbulent) viscosity is shown by v_t. P_a and ρ_0 stand for the atmospheric pressure and water reference density, respectively. *S* is the value of point source discharge; v_s and u_s are the water velocity induced by the point sources along *x* and *y* directions. F_v and F_u are the horizontal stress terms that are expressed as:

$$F_u = \frac{\partial}{\partial x}\left(2A\frac{\partial u}{\partial x}\right) + \frac{\partial}{\partial y}\left(A\left(\frac{\partial u}{\partial y} + \frac{\partial v}{\partial x}\right)\right) \tag{4}$$

$$F_v = \frac{\partial}{\partial y}\left(2A\frac{\partial v}{\partial y}\right) + \frac{\partial}{\partial x}\left(A\left(\frac{\partial u}{\partial y} + \frac{\partial v}{\partial x}\right)\right) \tag{5}$$

In the above relation, *A* indicates the horizontal eddy viscosity.

- Salinity advection-dispersion equation

$$\frac{\partial s}{\partial t} + \frac{\partial us}{\partial x} + \frac{\partial vs}{\partial y} + \frac{\partial ws}{\partial z} = F_s - \frac{\partial}{\partial z}\left(D_v\frac{\partial s}{\partial z}\right) + \widehat{H} + s_s S \tag{6}$$

where, D_v is the vertical turbulent (eddy) diffusion coefficient, $\widetilde{H}$ is a source component arising from atmospheric temperature changes, s_s is point source salinity, F_s is the component of horizontal salinity diffusion that is expressed by:

$$F_s = \left[\frac{\partial}{\partial x}\left(D_h\frac{\partial}{\partial x}\right) + \frac{\partial}{\partial y}\left(D_h\frac{\partial}{\partial y}\right)\right](s) \tag{7}$$

where D_h stands for horizontal eddy diffusion.

3.2. Model configuration

The first requirement for setting up a 3D model is importing topographical data for cell mesh generation into the model. A combined mesh generation technique is applied to the problem solution domain to reduce the execution time of the model and to foster fewer instabilities (DHI, 2017). Two flexible rectangular and triangular grids are implemented to superimpose horizontal grids onto the solution domain. The river channel is discretized with high-density rectangular grids (50×200 m) and triangular grids, consisting of 7238 elements and 4773 nodes, spread over the reservoir's surface (Fig. 2). Within the reservoir, as it goes deeper, the grids get denser to account for the extreme salinity gradient at lower elevations more accurately.

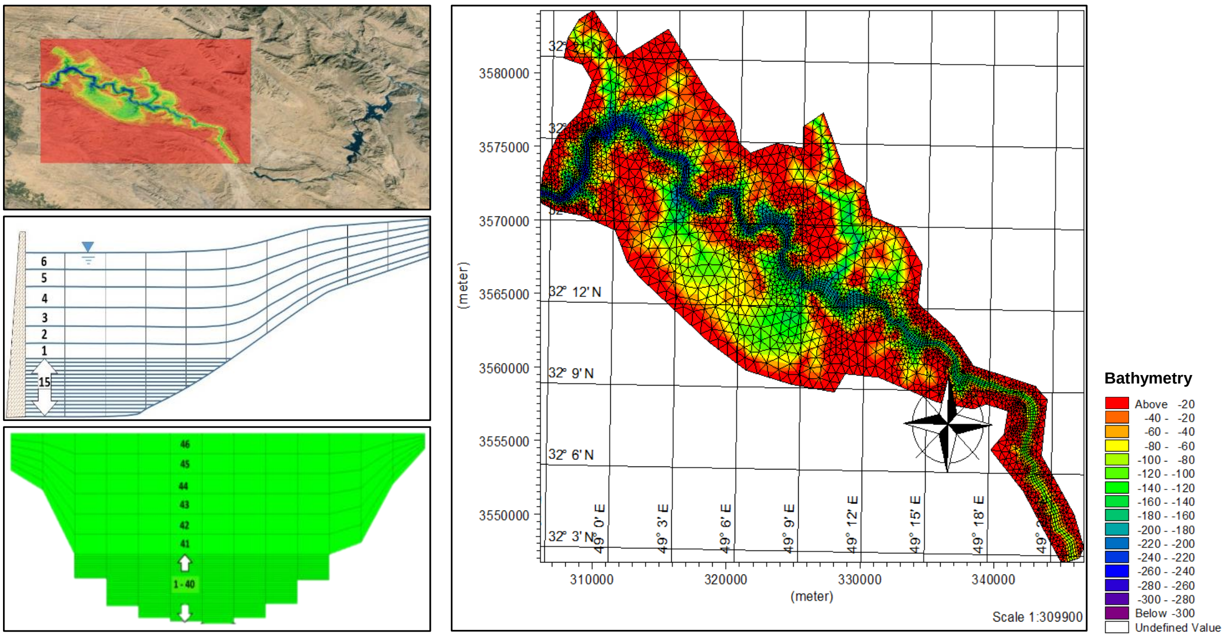

Figure 2. Horizontal (i.e., longitudinal and lateral) and vertical mesh generation of the Gotvand dam reservoir.

For vertical mesh generation of the solution domain of 46 deep layers, a combination of 40 Z-Level and 6 Sigma layers of the same thickness was designated. In deep Sigma mesh generation, layer thickness at different points varies depending on the rise and fall of the bottom, while Z-Level mesh generation has a constant thickness (Naderkhanloo, 2013; DHI, 2017). As the main flow course is along the river, the reservoir gets wet and dry sporadically during the impoundment, and the flow constantly fluctuates.

3.3. Measurement data and boundary/initial conditions

For setting up the MIKE3 mathematical model, some measured hydrological, climatological, topographical, and water quality data are required (see Table 1). In our study, these data were collected, validated, and prepared to be introduced to the model, which involved considerable time, financial resources, and high-tech devices. Salinity and water temperature data were gathered periodically using an electromechanical device with various sensors. The sensors were positioned at elevations of 80, 90, 95, 100, and 120 m above sea level for almost the first year of impoundment, from 23/7/2011 to 18/6/2012.

Table 1. Primary measurement data used in the three-dimensional (3D) model (MIKE3).

Parameter/Input	Reference
Reservoir bathymetry (topography)	30 m resolution DEM
Air temperature Relative humidity Rainfall and evaporation Wind speed and direction	Gotvand synoptic station
Karun river discharge and salinity (upstream boundary	Gotvand hydrometric

condition)	station
Discharge and salinity of saline rivers entering the reservoir GEF properties	(MGCEC, 2012)
Reservoir salinity in various depths and times Reservoir water level	Direct measurement

Due to the substantially high storage capacity of the Gotvand dam reservoir and the selection of a multi-stage impoundment process for the examination of GEF behaviour, the impoundment conditions were facilitated with the aid of various upstream dams of the Gotvand (i.e., Karun 4, Karun 3, Abbaspour and Masjed Soleyman dams, respectively). On occasions of a multi-stage impoundment, the increase in the output of the mentioned dams boosted the process of raising the water surface elevation of the Gotvand reservoir. Considering that such a process was specially designed for the particular case of the Gotvand dam, it is formulated based on time periods and different volumetric water yields back to the dam. Nevertheless, initiations and suspensions of impoundment are a matter of great importance. In normal circumstances and other situations, multiple starts and stops are rare during impoundment. Considering this, supervisors and operators of the Gotvand dam monitored and controlled conditions of GEF dissolution and the reservoir water quality by resorting to a kind of impoundment with periodic timing, time range, and variable volume. At each stage and provided that the situation was risk-free, they planned for the subsequent impoundment and its magnitude, both in time and volume. Given that the impoundment of the Gotvand reservoir was started in July 2011, and the monthly average discharge of the Karun River into the Gotvand reservoir in this month was 250 m^3/s (Fig. S4), this discharge value was used to set out the initial condition of the model before the start of impoundment.

The average salinity of the Karun river at the dam location before the impoundment was considered 1000 μmhos/cm, equal to the historical salinity of the river (MGCEC, 2012; Jalali et al., 2019). Impoundment of the dam began on 28/07/2011 and progressed through four stages up to 140, 160, 185, and 205 m. The reservoir's inflow and the bottom outlet discharge were set up to match the upstream and downstream boundary conditions during the impoundment period. The tributaries' average discharge and salinity were introduced to the model as point sources of salinity (Table S2 and Fig. S1).

3.4. Introduction of the GEF into the model

Since the MIKE3 model only accepts the point source option, we introduced the nonpoint source pollution of GEF to the model as a collection of point sources. In this regard, 945 point sources were considered over the entire evaporite formation interface (see Fig. S3), leading to the spatially varying dissolution rate of the GEF. Each point source required two characteristics for input into the model: the discharge and concentration; however, only the mass loading rate was available. Therefore, we included a hypothetical discharge and then divided the mass loading rate by the hypothetical discharge to calculate the source concentration. Then, we eliminated the hypothetical discharge effect (because no flow from evaporate formations enters the dam reservoir) by considering a source with a negative discharge (actually a sink) and a zero concentration. In this way, we successfully modelled the mass loading rate from the entire evaporite formation interface.

3.5. Model calibration and validation

Our in-situ measured salinity and water temperature data were collected from 28/07/2011 to 19/06/2012 for 327 consecutive days. Data from some elevations (i.e., 80 and 120 m) were used for calibration, while data from other elevations (i.e., 90, 95, 100, and 160 m) were employed for the numerical model validation. Then, the calibrated and validated model was used to simulate salinity in the Gotvand reservoir from 28/07/2011 to 02/18/2015 for 1332 days.

The roughness coefficient value was verified using the measured water elevation in the reservoir, available from 28/07/2011 to 21/05/2013 for 664 consecutive days. Along the length of the reservoir (from the beginning of the solution domain to the dam axis), three different values of bottom roughness, which also represent the Manning coefficient, were applied for sensitivity analysis. In addition to the bottom roughness and Manning coefficients, other hydrodynamic parameters were selected to analyse the model sensitivity, like time step, flood and dry depth, eddy viscosity, and dispersion coefficient.

The GEF dissolution rate calibration plays a crucial role in reservoir salinity simulation. The effect of hydrodynamics, salinity and temperature gradients, pH, hydraulic pressure, and heterogeneity of the masses within the reservoir contribute to the complexity of the GEF dissolution. Hence, simple relations and dissolution rates in previous studies are case-dependent and cannot be generalised elsewhere (Tavoosi et al., 2022). Accordingly, we calibrated the changes in the GEF dissolution rate by comparing the measured data of the reservoir salinity with modelling results. The measured salinity data at elevations of 80 and 120 meters were used for calibrating the model, and the measured salinity data at elevations of 90, 95, 100, and 160 meters were used for validation.

4 Reservoir management strategies

According to measurements, the salinity value entering the Gotvand dam reservoir is around 1000 μmhos/cm. As discussed, this salinity value represents the average historical salinity of the Karun River before the dam construction. Therefore, the dam's outlet water quality control (outlet loading) must be closely monitored to prevent salinity accumulation and role-playing of the GEF (in addition to salinity entering the reservoir from upstream) in the Gotvand dam reservoir after impoundment. In terms of implementation and operation, any salinity concentration is considered an outlet salinity that can be released. However, these values should be logically balanced to mitigate and control downstream damaging effects and avert incremental salinity accumulation in the dam reservoir. The release of the same salinity at 1000 μmhos/cm over time leads to excessive salinity accumulation in the dam reservoir due to submerged GEF dissolution. If this volume of salinity increases, output water becomes saline, and sluices and outlet structures will face some problems. As a result, values higher than the above should be considered as loading output under technical and control considerations. Then, continuous monitoring can prevent any possible environmental and structural problems in the future.

Overall, a safe value of salinity should be guided downstream. This value needs to account for the effects of both upstream salinity and salinity induced by the GEF submergence. Therefore, some salinity caused by the GEF should be added to upstream salinity. Then, the state of accumulated salt in the reservoir needs to be inspected. Here, three scenarios for behavioural investigation of accumulated salts in the reservoir—which itself is affected by the dam's salinity outlet—are explored, and their details are given below.

Conveying good-quality water downstream while paying particular attention to the qualitative conditions of the Gotvand dam and preventing salt accumulation is a complicated series of steps formulated within the framework of water salinity management in the reservoir. Even though this managerial aspect does not call for structural costs and undue physical interventions, it demands exact control plans, continuous monitoring of water salinity conditions from the reservoir to downstream, and following sensitive and decisive operational points. Consequently, employing the full structural capacity of the Gotvand and focusing on outlet water of varying volume and salinity can lead to the further success of this remedial strategy. Fig. 3 presents details of the type and elevation of Gotvand outlets. The dam has three outlets at different elevations, namely: bottom pipe or GRP pipe at 90 m elevation, lower outlet at 123 m elevation, and power plant inlets at 158 m elevation. It is also possible to convey water downstream via GRP pipe in water diversion tunnels at 110 m elevation (MGCEC, 2012). It is possible to simultaneously improve dam reservoir and downstream conditions by continuously utilising the limited or total capacity of these sluices, whether individually or integrally. Whereas lower reservoir elevations contain high salinity, upper elevations have a good water quality condition in terms of salinity—sometimes lower than the permissible limit. The only viable solution until the problem is completely resolved is to develop detailed plans for concurrently employing all these capacities.

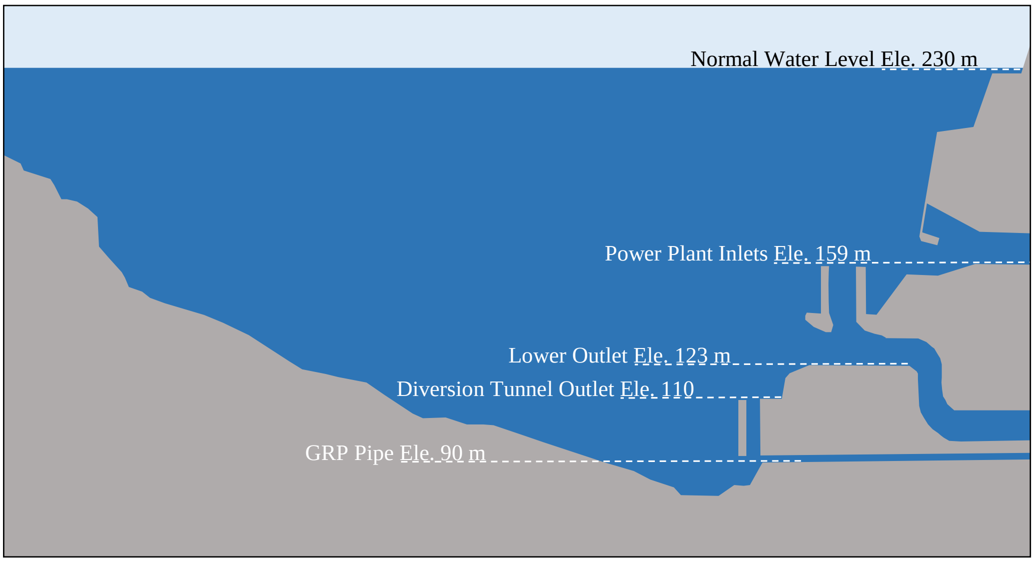

Figure 3. Schematic diagram of the outlets and their corresponding elevations in the Gotvand dam reservoir.

Here, the total outlet salinity loading is drawn up in three different scenarios: (i) 1200 µmhos/cm, (ii) 1300 µmhos/cm, and (iii) 1400 µmhos/cm, which are more than the upstream salinity (i.e., 1000 µmhos/cm). In each scenario, a constant value of salinity loading from all the outlets as the final salinity loads to the downstream are considered, as shown in Eqs. (8) and (9).

$$\mathrm{UL} + \mathrm{SFL} = \mathrm{PIL} + \mathrm{LOL} + \mathrm{BOL} \tag{8}$$

$$\mathrm{BO} = \mathrm{DTO} + \mathrm{GRP} \tag{9}$$

where, UL is the upstream loading, SFL is the GEF loading, PI is the power plant inlet, LO is the lower outlet, BO is the bottom outlet, DTO is the diversion tunnel outlet, and GRP is the GRP outlet at the lowest level.

5 Results and discussion

5.1. Results of salinity measurements in the Gotvand reservoir

With the submergence and GEF dissolution in the reservoir, the bottom layers at low elevations became increasingly saline. The salinity accumulation steadily continued from the reservoir bottom to the 90 m elevation within this process. After two months of impoundment, the water level reached an elevation of 140 m when a strong halocline was observed in the water column. Also, the measured salinity was very high at the monimolimnion (i.e., 94.1 and 42.8 ppt at 80 and 90 m elevations, respectively). In contrast, the upper layers were less impacted by salinity (salinity was 9, 1.7, and 0.4 ppt at 95, 100, and 120 m elevations, respectively). The salinity remained constant at the reservoir bottom (i.e., 80 m elevation), while incremental salinization started from 21/01/2012 and continued by the end of field measurements, i.e., 19/06/2012. Within this period, salinity at 90, 95, 100, and 120 m elevations increased to 94.6, 53.4, 28.2, and 5.1 ppt, respectively (Fig. 4a), causing a crenogenic meromixis condition in the Gotvand reservoir. Under this condition, the Gotvand reservoir was increasingly stratified because of the introduction of an uninterrupted source of saline water to the bottom layers of the lake resulting from GEF dissolution (Hutchinson, 1937; Tavoosi et al., 2022).

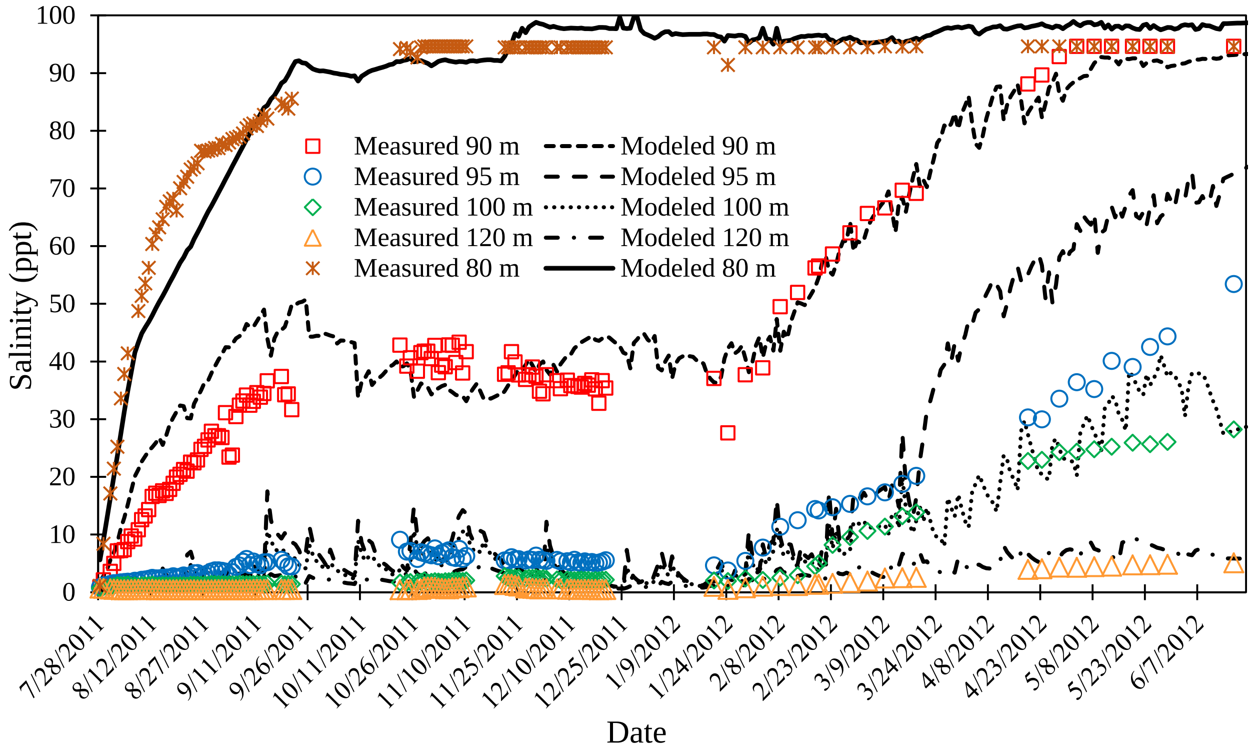

(a)

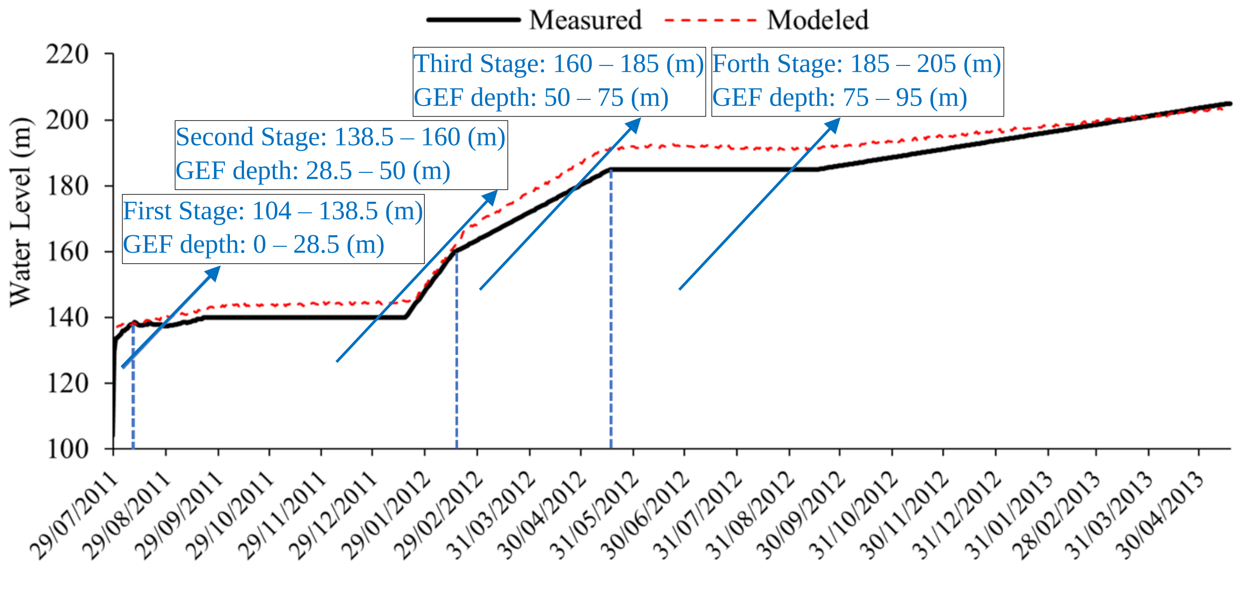

(b)

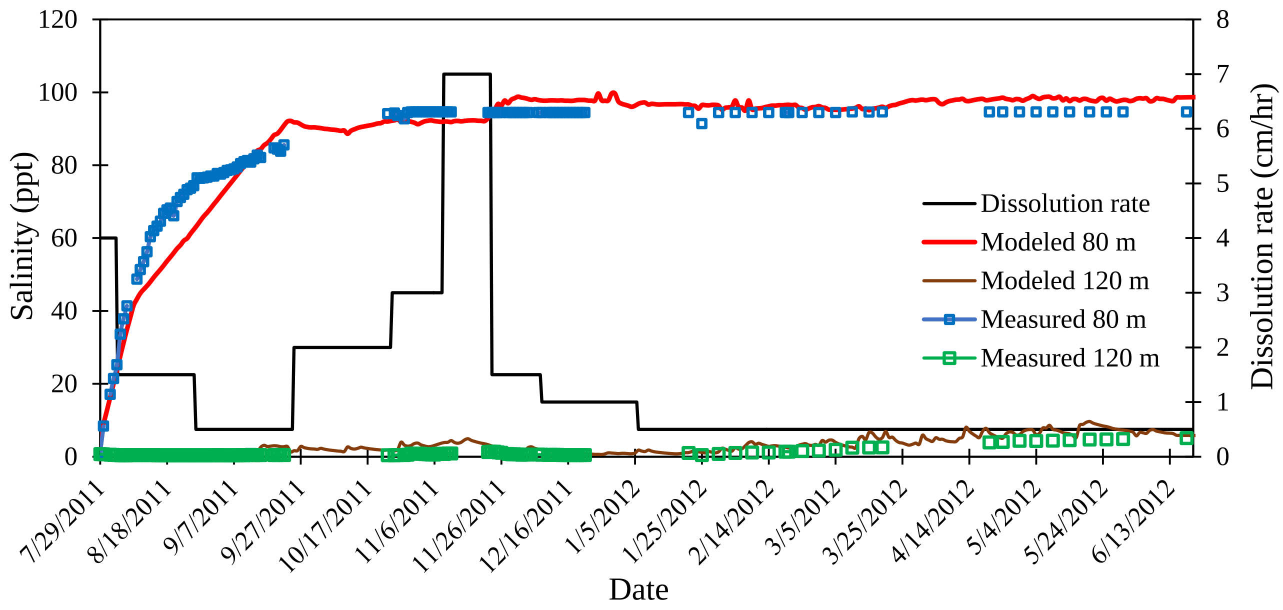

(c)

Figure 4. (a) Salinity calibration (elevations of 80 m and 120 m) and validation (elevations of 90 m, 95, and 100 m) results in the Gotvand dam reservoir from 28/07/2011 to 19/06/2012, (b) the measured and modelled water surface elevation in the Gotvand dam reservoir during the different impoundment stages, and (c) the measured and modelled salinity values at two elevations of 80 m and 120 m in the calibration stage and the corresponding calibrated dissolution rates of the Gachsaran evaporite formation (GEF).

5.2. Hydrodynamics calibration and validation results

Calibration results of water level elevation in the reservoir are shown in Fig. 4b, with a mean absolute error (MAE) of 3.62 m. As shown in Fig. 4b, the MIKE3 model overestimates the water levels in the Gotvand reservoir with relatively considerable differences between the simulated and observed water levels. Sparse temporal frequency data with short duration could create many challenges for hydrodynamic simulations, especially in the case of the Gotvand dam that is confidential with few available data. However, the simulated results appropriately follow the available trend in the measured water level. Also, the calibrated bottom roughness and Manning coefficients along different lengths of the reservoir are presented in Table 2. The simulation results were not highly sensitive to other parameters due to the reservoir's relatively low flow velocity and the accuracy of the sensitivity analysis. Therefore, the previously recommended values for calibration parameters were used (see Table 3).

Given that water temperature is one of the influencing factors on the density value, which also affects the hydrodynamics of the reservoir, we investigated the depth profiles of simulated water temperature against those measured in the depth of the Gotvand reservoir. Our results revealed only one annual mixing in the reservoir during cold months, mainly December to March, putting the reservoir in a warm monomictic state (Noori et al., 2019). The MAE values for water temperature calibration and validation were 2.2 °C and 3.6 °C, respectively.

Table 2. Calibrated values of the bottom roughness and Manning coefficients during the impoundment period of the Gotvand dam reservoir.

Parameter	Longitudinal distance (km)

	0-30	30-60	60-90
Manning coefficient	0.03	0.035	0.04
Bottom roughness coefficient	0.196	0.494	1.1

Table 3. Recommended values for the calibration parameters of the MIKE3 model used in our study.

Parameter name	Explanations	Value	
Time step	Based on test results of the independence of the time steps	1 (hour)	
Flood and dry a: Drying depth b: Wetting depth c: Flooding depth	Based on calibration and the DHI advise	DHI advise a = 0.005 (m) b = 0.05 (m) c = 0.1 (m)	Calibrated a = 0.05 (m) b = 0.07 (m) c = 0.1 (m)
Eddy viscosity a: Horizontal eddy viscosity b: Vertical eddy viscosity	a: Based on the DHI advise and solution status (the Smagorinsky formulation) b: Based on the DHI advise and solution status (the log law formulation)	DHI advise a = 0.1 to 0.3 b = 0.1 to 0.4 (m^2/sec)	Considered a = 0.1 b = 0.1 (m^2/sec)
Dispersion a: Horizontal dispersion b: Vertical dispersion	a: Based on the DHI advise and solution status (a ratio of horizontal eddy viscosity) b: Based on the DHI advise and solution status (a ratio of vertical eddy viscosity)	a = 0.01 × Horizontal eddy viscosity (m^2/sec) b = 0 (m^2/sec)	

5.3. Dissolution rate calibration results

Contrary to similar studies (e.g., Aghasian et al., 2019; Tavoosi et al., 2022), calibration results revealed that the dissolution rate varied depending on the different impoundment periods. The lowest value was 0.5 cm/h, while the highest was 7 cm/h (Fig. 4c). Overall, the most decisive factor responsible for this range of dissolution rate variations in the Gotvand dam is hydrodynamic flow changes in the reservoir. Based on 3D changes induced by various stages of impoundment, the dissolution rate is variable until it reaches 0.5 cm/hr, primarily because the water surface in the reservoir reaches the designed elevation, and the entirety of the GEF gets submerged. While we did not investigate the influence of other factors on the GEF dissolution rate (e.g., pH, water temperature, and salt saturation concentration) (Raines and Dewers, 1997; Lasaga, 1998; Jeschke et al., 2001; Mbogoro et al., 2011; Lebedev, 2015), we hypothesised that a change in these factors during the Gotvand dam impoundment could contribute to the temporal variation of the dissolution rate.

5.4. Salinity calibration and validation results

The MAE values for salinity calibration and validation were 1.9 and 3.2 µmohs/cm, respectively. Given the large variation of salinity in the Gotvand dam reservoir (up to 100,000 µmohs/cm in deep layers), the calculated MAE values are satisfactory. Also, the simulated depth profiles of salinity appropriately follow the measured salinity profiles in the Gotvand reservoir (Fig. 4a). Accordingly, the MIKE3 model simulates salinity in the Gotvand dam reservoir more accurately than water temperature. Sparse temporal frequency data with short duration could reduce the salinity calibration accuracy, especially in the case of the Gotvand dam that is confidential with few available data. In addition, complex nature of the reservoir and outcropped GEF, the complexity of the problem-solving environment, and the arrangement and introduction of GEF to the 3D model could reduce the salinity calibration acuraccy in the Gotvand hypersaline reservoir.

Salinity and temperature gradients in the reservoir depth are almost inversely correlated. It is evident that the salinity gradient at the bottom of the reservoir is very high, as demonstrated by the measurement data (Fig. 4a). Thus, we introduced thinner layers at the bottom of the reservoir to improve the accuracy of salinity simulations. Due to the thermocline, the water temperature gradient in the bottom layers (hypolimnion) is very low. Consequently, the bottom layers should be coarser than those in the surface and middle layers. As a result, the number of vertical layers should be increased to capture both salinity and temperature gradients accurately. This process exponentially increases the model calculation time, which is considered a main obstacle in hydrodynamics and salinity simulation in a large and deep reservoir such as the Gotvand dam reservoir. Since salinity concentration was our target parameter, we only increased the number of bottom layers. However, it should be noted that this layering arrangement allowed us to capture the water temperature gradients in the depth of the reservoir adequately with an overall acceptable AME, as discussed before.

5.5. Salinity stratification and accumulation

The GEF gets dissolved due to increased water surface elevation from the early impoundment. By generating density current and moving forward, the densely dissolved GEF settled on the lower layers of the reservoir. This process led to salinity accumulation up to the elevations of 80 and even 90 m for three months. As water surface elevation remained constant for four months, the GEF dissolution rate declined, and the current low dissolution rate merely maintained the salinity of all elevations. Re-impoundment of the dam on 21/01/2012—in other words, an increase in water surface elevation and inlet-outlet flows during February and March—heightened the GEF dissolution and led to salinity accumulation and escalation at upper reservoir elevations (Fig. 4a). It is noteworthy that, at the end of the period and near the reservoir bottom, the salinity was around 100 ppt, which is virtually three times higher than that of the high-seas. In sum, MIKE 3 simulation results show a crenogenic meromictic condition started in the reservoir from its beginning impoundment which remained stable during the study period, even December to March when the Gotvand reservoir is homo-thermal. In other words, the Gotvand reservoir is stratified chemically due to a continuous source of dissolved GEF in the deep layers of the reservoir. The salinity gradient in the water column shaped the mixolimnion and monimolimnion in the top and deep layers, respectively. Both layers are disconnected by a distinct halocline that contributes to different salt concentrations in the bottom and surface layers in the reservoir (Fig. 4a). Therefore, deep hypersaline layers in the reservoir do not simply mix with the surface layers using external forces such as extreme floods. For example, our simulation results revealed that the halocline prohibits the mixing between deep and surface layers, even under the condition of a 1000-year flood as inflow to the reservoir, which is consistent with the reported results for 100-year and 1000-year floods in another salinized reservoir (Tavoosi et al., 2022).

Figure 5 shows graphs of salinity loading caused by GEF dissolution in the reservoir (from the first stage of the impoundment to the last stage) and accumulated salt in the reservoir (observed and simulated by the 3D mathematical model). In light of the configuration and accuracy of the 3D mathematical model, seamless compatibility was established between the observed values of accumulated salt in the reservoir and simulated ones. Moreover, the salinity accumulation pattern in the reservoir was obtained over a more extended period by extrapolating and using the results of the 3D simulation from the end of the simulation period (dashed line diagram). This pattern is approximately a linear process increasing over time. Based on the observed values of accumulated salt in the reservoir, the linear process demonstrated good consistency, reflecting the generalisation accuracy of the simulated trend.

With the complete submergence of the GEF and from the end of the last impoundment period to 25/02/2015, a constant loading induced by the total impact of these masses was observed (thin red diagram in Fig. 5). The underlying cause of the constant loading is dissolution rate stabilisation, which is caused by two main factors: the complete submergence of the GEF due to large-volume impoundment and reduction in salinity difference between adjacent layers (Tavoosi et al., 2022). Qualitative observations and measurements in the reservoir confirm the authenticity of dissolution rate stabilisation. A look at Fig. 5 also reveals the occurrence of multiple peaks in the diagram of salt masses loading. These simulated peaks correspond to the different impoundment stages of the reservoir (four stages). The more the volume and time length of impoundment, the bigger the peaks of salt masses loading. On the other side, during periods when the impoundment's volume and time length decreased, the loading diagram dropped further. As discussed earlier, the reason behind the multi-stage impoundment with this frequency and volume is to study the behaviour of GEF in contact with the dam reservoir.

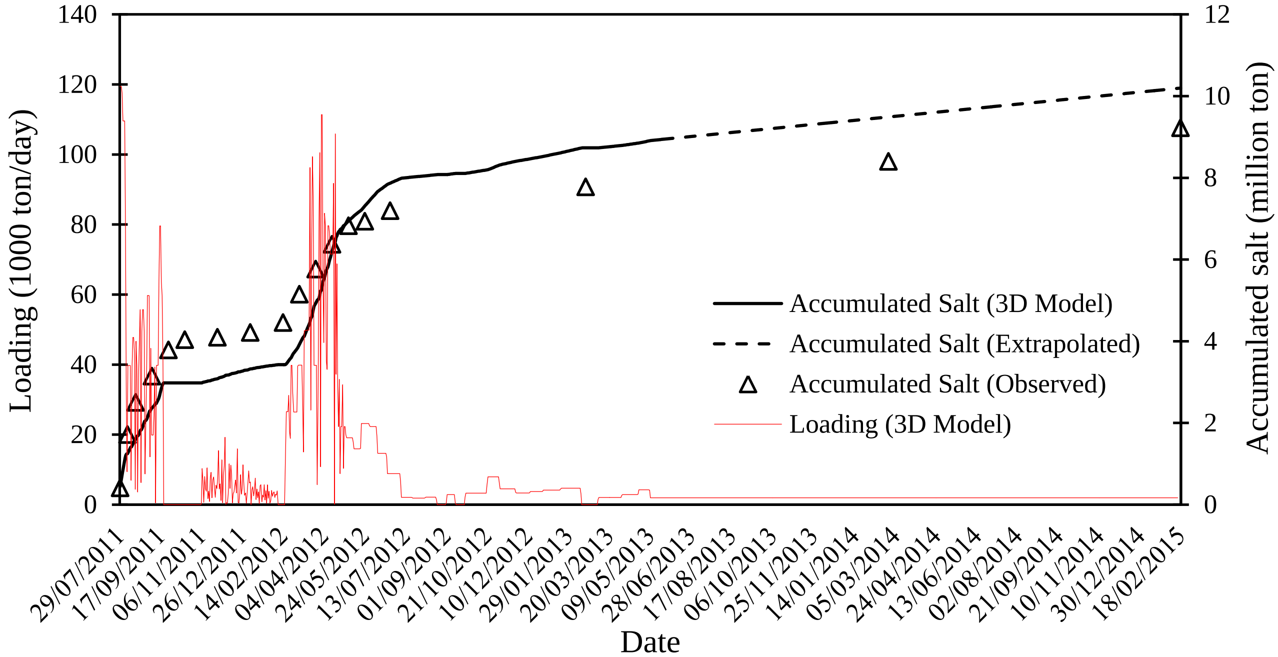

Figure 5. The process and values of salt accumulation (observed and modelled) and the diagram of salt masses loading for 43 months in the Gotvand dam reservoir.

5.6. Evaluation of reservoir management strategies

Here, a summary of scenarios is presented to better understand the salinity evolution in the Gotvand reservoir. In each scenario, a constant value of the loading outlet, which is the final salinity outlet targeted for downstream delivery, is considered. This constant value is the sum of inlet upstream salinity and salinity caused by GEF submergence. There are three different scenarios for the loading of outlet salinity: 1200, 1300, and 1400 µmhos/cm. In this respect, the outlet salinity value in all scenarios was determined based on expert observations and frequent problem-solving meetings. More importantly, maximum historical downstream salinity was considered to protect downstream targets from salinity hazards. In addition, tolerance of downstream targets to the determined salinity—relative to different uses, mainly agricultural—is another reason for assigning the mentioned value. Nevertheless, the mentioned salinity outlet should be carried out using integrated water extraction from various layers to ensure that the amount of inlet/outlet salts is balanced.

In the first scenario, the outlet salinity value (outlet loading) is 1200 µmhos/cm, slightly more than that of the inlet from upstream, i.e., 1000 µmhos/cm. Figure 6a shows the total loading in the Gotvand reservoir (total upstream and salt masses loadings) by a thin red line. Furthermore, inlet accumulative salinity mass values in the reservoir (thick red line) and outlet accumulative salinity mass values heading downstream (thick blue line) are demonstrated. On the other hand, the value of outlet salinity loading from the reservoir had been 1000 µmho/cm since the beginning of impoundment to a specific period. By the end of the last impoundment stage, it added up to 1200 µmho/cm, as shown by a dashed blue line diagram. This diagram analyses the effect of applying an outlet loading of 1200 µmho/cm. Minor differences in the slopes of accumulative diagrams indicate no salinity accumulation in the reservoir.

Similar explanations are valid for the second and third scenarios. The difference is that the values of outlet loading from the sluices installed in the dam body to downstream for the second and third scenarios are correspondingly 1300 and 1400 µmhos/cm. Figures 6b and 6c, illustrate the results of accumulated salt under these scenarios. Evidently, if the value of outlet loading increases, the slope of the downstream salinity accumulation diagram also increases.

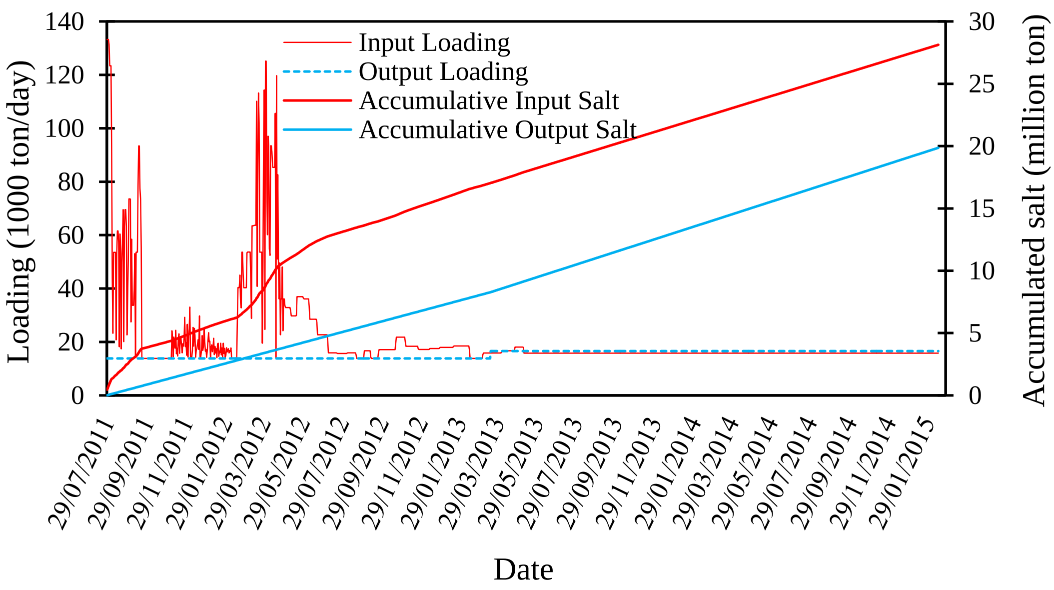

(a)

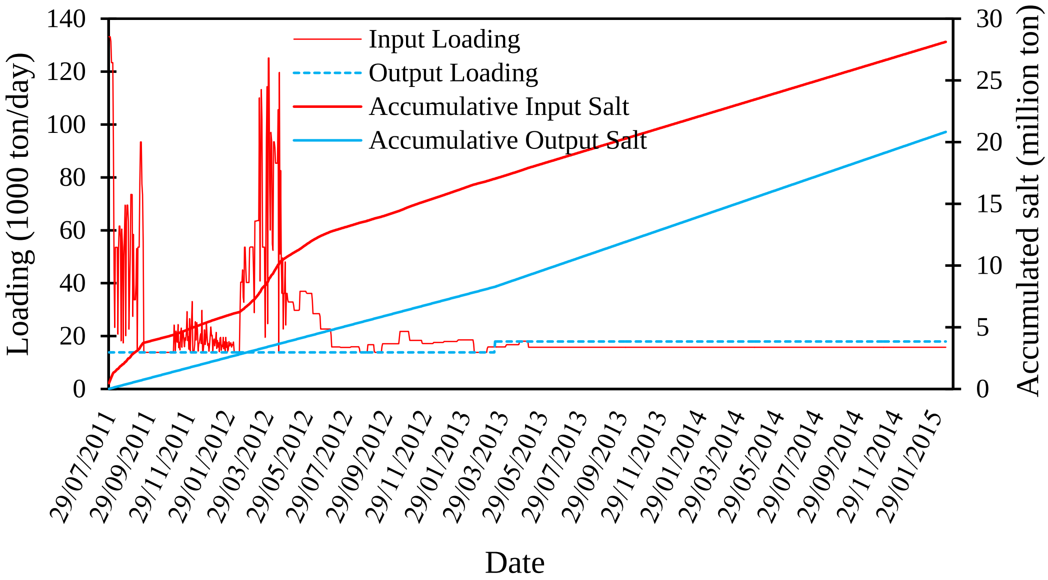

(b)

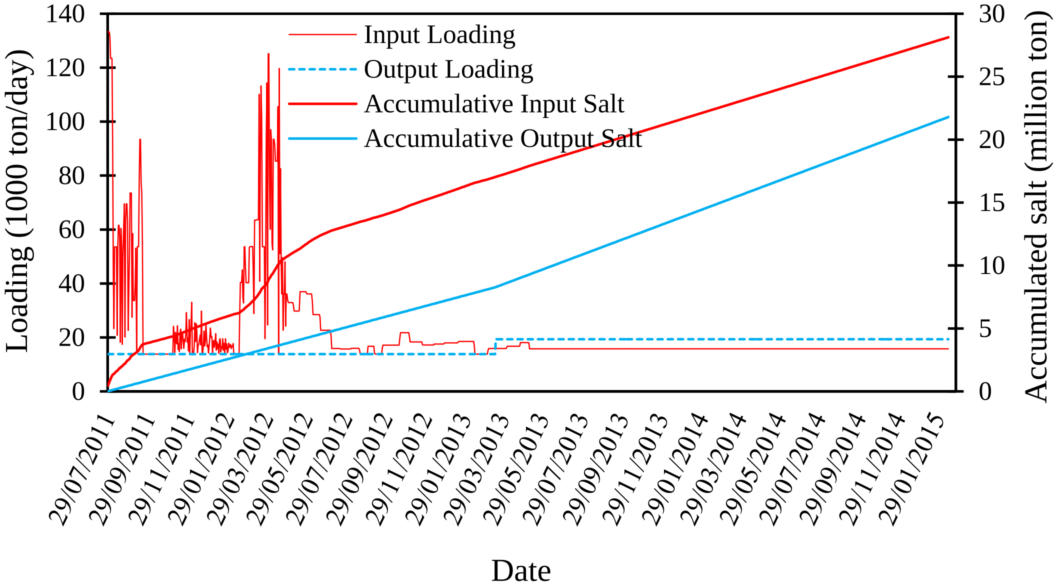

(c)

Figure 6. Loading and accumulative values of inlet/outlet salt mass in the Gotvand Dam reservoir under different scenarios of outlet salinity management: (a) 1200 µmhos/cm, (b) 1300 µmhos/cm, (c) 1400 µmhos/cm.

The above figures vividly illustrate that the difference in inlet/outlet accumulative salt mass values remains in the reservoir as final accumulated salt. Concerning the limitation in increasing the downstream outlet loading, the ultimate objective of presenting various scenarios is to lower the final value of accumulated salt in the reservoir over time. Under these circumstances, having precise information on salt mass allows us to estimate the time of the complete dissolution of the GEF in the dam reservoir and the time of the return of the dam to normality. Furthermore, obtaining accurate information about the outlet loading value can help resolve the problem of salt accumulation in the reservoir appropriately and logically. Overall, these estimations are a managerial instruction to monitor the reservoir salinity continuously and meticulously until the problem is resolved. In this regard, Fig. 7 displays the effect of applying all the scenarios and prospects. As illustrated in the figure, an appropriate increase in outlet loading reduces the final accumulated salt mass in the reservoir. The effect of each scenario on the final accumulated salt in the dam reservoir is shown in three different diagrams. Here, the effect of applying each scenario on the diagram of accumulated salt is shown by time-weighted lines with negative slopes. When the relevant scenario is applied, the descending trend of each line arrives at the lowest value of accumulated salt.

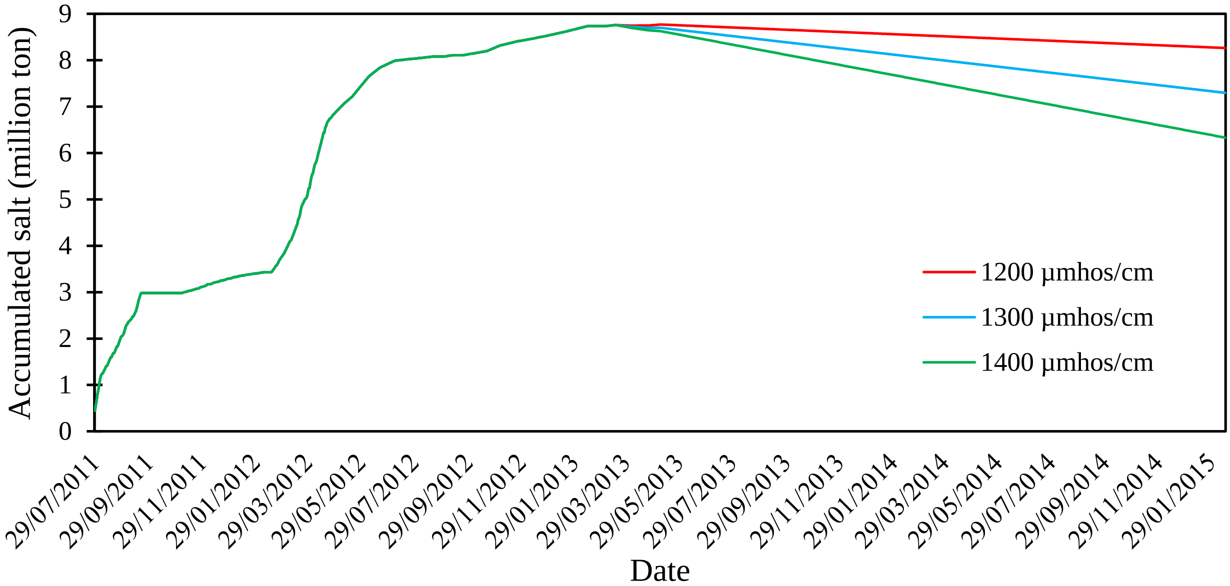

Figure 7. The temporal process of salt accumulation inside the Gotvand dam reservoir in the first, second, and third scenarios.

Considering the limited volume of evaporite formations in the Gotvand reservoir area, the proposed scenarios aim to ensure that the salt inlet and outlet balance reduces the accumulated salt in the reservoir (Fig. 7). Consequently, the accumulated salt in the reservoir will gradually be removed over the coming years (2040s), and the reservoir will have the same conditions as other normal dam reservoirs. It should be noted that the mentioned years may be affected because of uncertainty related to the real volume of GEF (about 300 million m^3). As a useful suggestion, it is beneficial to monitor the accumulated salt in the reservoir throughout the dam's lifespan due to its specific conditions. This will ensure that the accumulation rate is negative. In other words, the reservoir gets closer to the conditions of a normal reservoir.

5.7. Uncertainties

Our proposed scenarios for the salinity management in the Gotvand dam reservoir depends on various factors, including the nature of the reservoir and the Karun river system (including all upstream and downstream components), the tolerance and response of all downstream components to the proposed scenarios, the ability of available tools and facilities, as well as the technical, hardware, and operator status of the Gotvand dam. The way to propose these scenarios is actually based on the findings of this study and field facts (especially in the initial years of the dam impoundment), available measured data, and advanced mathematical modeling. For example, the findings of this study show that removing salt from the reservoir under proposed scenarios will eventually improve the condition of the reservoir over the coming years (2040s) compared to the first years following the impoundment. In this case, the accumulated salt at the bottom of the reservoir will be removed and the dam's salinity crisis will rectify. However, the important thing is, something else is going on in reality. So far the salinity management of the reservoir has been based on operational experiences. According to unpublished reports, the salinity management scenarios have varied between EC =250 and 1950 µmhos/cm from 2011 to 2021. This means that there is a significant difference between the salinity management scenarios proposed by our research and what is being currently applied. This difference causes ambiguity in imagining the future salinity crisis in the reservoir by applying the implemented salinity management scenarios. In addition, lack of adequate access to comprehensive and up-to-date salinity data in the reservoir limits the capacity and scope of precise scientific studies about the future conditions of the Gotvand dam reservoir, and our research is no exception. As discussed in detail, what has made this research important is providing an optimal solution to solve the salinity crisis in the Gotvand dam reservoir with regard to minimal access to measured data and relying on advanced mathematical modeling. Finally, as to whether the proposed scenarios and solutions can be applied in reality is a decision that needs to be followed up and adopted by officials and the management team of the Gotvand dam

6. Conclusion

Outcropped salty geological formations within the reservoir's area significantly affect reservoir water quality, dam structures, and downstream ecosystems, which may sometimes inhibit dams from fulfilling their functions. Therefore, reservoir salinity management is required to mitigate the negative impacts of water quality and possible consequences for downstream environments. The present study proposed a salinity management strategy for the Gotvand dam, where the submergence of large salt masses due to the reservoir impoundment made the reservoir water increasingly saline. In this regard, time-weighted measures were taken to provide an exact calculation of salinity stratification in the reservoir using a 3D numerical model. Various scenarios were implemented to determine the most appropriate value of downstream outlet loading to reduce salinity accumulation in the reservoir and protect the downstream environment from salinity hazards. Simulation results indicate that the reservoir salinity management technique may effectively control the existing salinity crisis. Our suggested method can be viewed as a viable approach by relevant managers and officials for salinity management in the Gotvand reservoir, the world's most saline dam reservoir.

Competing interests

The authors declare no competing interests.

Author Contributions

Conceptualization: Siamak Amiri, Mehdi Mazaheri, Vahid Naderkhanloo, Jamal Mohammad Vali Samani. **Methodology:** Siamak Amiri, Mehdi Mazaheri, Vahid Naderkhanloo, Jamal Mohammad Vali Samani, Roohollah Noori. **Data curation:** Siamak Amiri, Mehdi Mazaheri, Vahid Naderkhanloo, Jamal Mohammad Vali Samani. **Formal analysis:** Siamak Amiri, Mehdi Mazaheri, Vahid Naderkhanloo. **Investigation:** Siamak Amiri, Mehdi Mazaheri, Vahid Naderkhanloo, Jamal Mohammad Vali Samani, Roohollah Noori. **Resources:** Mehdi Mazaheri, Jamal Mohammad Vali Samani. **Software:** Siamak Amiri, Mehdi Mazaheri, Vahid Naderkhanloo. **Supervision:** Mehdi Mazaheri, Jamal Mohammad Vali Samani, Ali Torabi Haghighi, Roohollah Noori. **Validation:** Siamak Amiri, Mehdi Mazaheri, Vahid Naderkhanloo, Roohollah Noori. **Visualization:** Siamak Amiri, Mehdi Mazaheri, Vahid Naderkhanloo, Jamal Mohammad Vali Samani, Roohollah Noori. **Writing – original draft:** Siamak Amiri, Mehdi Mazaheri, Vahid Naderkhanloo. **Writing – review & editing:** Siamak Amiri, Mehdi Mazaheri, Vahid Naderkhanloo, Jamal Mohammad Vali Samani, Sahand Ghadimi, Ali Torabi Haghighi, Roohollah Noori.

Data Availability Statement

Data used in our study are included in a “Zenodo” repository, available through https://doi.org/10.5281/zenodo.8403987.

References

Aghasian, K., Moridi, A., Mirbagheri, A., & Abbaspour, M. (2019). Selective withdrawal optimization in a multipurpose water use reservoir. *International Journal of Environmental Science and Technology*, 16(10), 5559-5568. https://doi.org/10.1007/s13762-019-02363-x

Bedri, Z., Corkery, A., O'Sullivan, J.J., Alvarez, M.X., Erichsen, A.C., Deering, L.A., et al. (2014). An integrated catchment-coastal modelling system for real-time water quality forecasts. *Environmental Modelling & Software*, 61, 458-476. https://doi.org/10.1016/j.envsoft.2014.02.006

Best, J. (2019). Anthropogenic stresses on the world’s big rivers. *Nature Geoscience*, 12(1), 7-21. https://doi.org/10.1038/s41561-018-0262-x

DHI (Danish Hydraulic Institute). (2017). Scientific Documentation, MIKE21 & MIKE3 Flow Model FM - Hydrodynamic and Transport Module. Danish Hydraulic Institute, Horsholm, Denmark. https://manuals.mikepoweredbydhi.help/2017/Coast_and_Sea/MIKE_321_FM_Scientific_Doc.pdf

Fakouri, B., Mazaheri, M., & Samani, J.M. (2019). Management scenarios methodology for salinity control in rivers (case study: karoon river, Iran). *Journal of Water Supply: Research and Technology-Aqua*, 68, 74-86. https://doi.org/10.2166/aqua.2018.056

Hutchinson, G.E. (1937). A contribution to the limnology of arid regions primarily based upon observations made in the Lahontan Basin. Trans. Conn. Acad. Arts Sci., 33, pp.37-142.

IPRC (Islamic Parliament Research Center). (2011). An Investigation of the effects of Gachsaran-e-Anbal formations in the Gotvand Dam reservoir on the water quality of Karun River and the salinity of the dam reservoir (In Persian).

IWPRDC (Iran Water and Power Resources Development Company). (2011). Report of Gotvand Dam and Power Plant Design (In Persian).

Jalali, L., Zarei, M., & Gutiérrez, F. (2019). Salinization of reservoirs in regions with exposed evaporites. The unique case of Upper Gotvand Dam, Iran. *Water Research*, 157, 587-599. https://doi.org/10.1016/j.watres.2019.04.015

Jeschke, A.A., Vosbeck, K., Dreybrodt, W., 2001. Surface controlled dissolution rates of gypsum in aqueous solutions exhibit nonlinear dissolution kinetics. Geochim. Cosmochim. Acta 65 (1), 27–34. https://doi.org/10.1016/S0016-7037(00)00510-X

Kerachian, R., & Karamouz, M. (2007). A stochastic conflict resolution model for water quality management in reservoir–river systems. *Advances in Water Resources*, 30(4), 866-882. https://doi.org/10.1016/j.advwatres.2006.07.005

Kheirabadi, H., Noori, R., Samani, J., Adamowski, J.F., Ranjbar, M.H., & Zaker, N.H. (2018). A reduced-order model for the regeneration of surface currents in Gorgan Bay, Iran. *Journal of Hydroinformatics*, 20(6), 1419-1435. https://doi.org/10.2166/hydro.2018.149

Lasaga, A.C., 1998. Kinetic Theory in the Earth Sciences. Princeton University Press, Princeton.

Lebedev, A.L., 2015. Kinetics of gypsum dissolution in water. Geochem. Int. 53 (9), 828–841. https://doi.org/10.1134/S0016702915070058

Malekmohammadi, B., Uvo, C.B., Moghadam, N.T., Noori, R., & Abolfathi, S. (2023). Environmental risk assessment of wetland ecosystems using Bayesian belief networks. *Hydrology*, 10(1), 16. https://doi.org/10.3390/hydrology10010016

Mbogoro, M.M., Snowden, M.E., Edwards, M.A., Peruffo, M., Unwin, P.R., 2011. Intrinsic kinetics of gypsum and calcium sulfate anhydrite dissolution: surface selective studies under hydrodynamic control and the effect of additives. J. Phys. Chem. C 115 (20), 10147–10154. https://doi.org/10.1021/jp201718b

MGCEC (Mahab Ghodss Consulting Engineering Company). (2012). Report of Gotvand Dam and Power Plant (In Persian).

Monjezi, S., Najarchi, M., Mo'meni, M., Monjezi, N., & Hassuninezade, H. (2021). Simulation of salinity distribution of Anbar Salt Dome in Gotvand Reservoir in Iran, using system dynamics and proposes a strategy to reduce salinity. *Water Resources*, 48(6), 1013-1022. https://doi.org/10.1134/S009780782106018X

Mulligan, M., van Soesbergen, A., & Sáenz, L. (2020). GOODD, a global dataset of more than 38,000 georeferenced dams. *Scientific Data*, 7(1), 1-8. https://doi.org/10.1038/s41597-020-0362-5

Naderkhanloo, V. (2013). Three- Dimensional modeling of hydrodynamic and salinity of Gotvand dam reservoir. https://parseh.modares.ac.ir/thesis.php?id=5172719&sid=1&slc_lang=En

Noori, R., Ansari, E., Bhattarai, R., Tang, Q., Aradpour, S., Maghrebi, M., et al. (2021). Complex dynamics of water quality mixing in a warm mono-mictic reservoir. *Science of The Total Environment*, 777, 146097. https://doi.org/10.1016/j.scitotenv.2021.146097

Noori, R., Asadi, N., & Deng, Z. (2019). A simple model for simulation of reservoir stratification. *Journal of Hydraulic Research*, 57(4), 561-572. https://doi.org/10.1080/00221686.2018.1499052

Noori, R., Woolway, R.I., Saari, M., Pulkkanen, M., & Kløve, B. (2022). Six decades of thermal change in a pristine lake situated north of the Arctic Circle. *Water Resources Research*, 58(9), e2021WR031543. https://doi.org/10.1029/2021WR031543

Poff, N.L., Brown, C.M., Grantham, T.E., Matthews, J.H., Palmer, M.A., Spence, C.M., et al. (2016). Sustainable water management under future uncertainty with eco-engineering decision scaling. *Nature Climate Change*, 6(1), 25-34. https://doi.org/10.1038/nclimate2765

Raines, M.A., Dewers, T.A., 1997. Mixed transport/reaction control of gypsum dissolution kinetics in aqueous solutions and initiation of gypsum karst. Chem. Geol. 140 (1–2), 29–48. https://doi.org/10.1016/S0009-2541(97)00018-1

Ranjbar, M.H., Etemad-Shahidi, A., & Kamranzad, B. (2020). Modeling the combined impact of climate change and sea-level rise on general circulation and residence time in a semi-enclosed sea. *Science of The Total Environment*, 740, 140073. https://doi.org/10.1016/j.scitotenv.2020.140073

Ranjbar, M.H., Etemad-Shahidi, A., Helfer, F., & Hamilton, D. (2022). Impacts of atmospheric stilling and climate warming on cyanobacterial blooms: An individual-based modelling approach. *Water Research*, 118814. https://doi.org/10.1016/j.watres.2022.118814

Simonovic, S.P., & Arunkumar, R. (2016). Comparison of static and dynamic resilience for a multipurpose reservoir operation. *Water Resources Research*, 52(11), 8630-8649. https://doi.org/10.1002/2016WR019551

Tavoosi, N., Hooshyaripor, F., Noori, R., Farokhnia, A., Maghrebi, M., Kløve, B., et al. (2022). Experimental-numerical simulation of soluble formations in reservoirs. *Advances in Water Resources*, 160, 104109. https://doi.org/10.1016/j.advwatres.2021.104109

Wang, H.W., & Kondolf, G.M. (2014). Upstream sediment-control dams: five decades of experience in the rapidly eroding Dahan River Basin, Taiwan. *Journal of the American Water Resources Association*, 50(3), 735-747. https://doi.org/10.1111/jawr.12141

Winton, R.S., Calamita, E. & Wehrli, B. (2019). Reviews and syntheses: Dams, water quality and tropical reservoir stratification. *Biogeosciences*, 16(8), 1657-1671. https://doi.org/10.5194/bg-16-1657-2019

Zaragüeta, M., & Acebes, P. (2017). Controlling eutrophication in a Mediterranean shallow reservoir by phosphorus loading reduction: the need for an integrated management approach. *Environmental Management*, 59(4), 635-651. https://doi.org/10.1007/s00267-016-0815-y

Ziemińska-Stolarska, A., & Kempa, M. (2021). Modeling and monitoring of hydrodynamics and surface water quality in the sulejów dam reservoir, Poland. *Water*, 13(3), 296. https://doi.org/10.3390/w13030296